Noiseless Optical Amplification of Images

Sang-Kyung Choi, Michael Vasilyev, and Prem Kumar*
Department of Electrical and Computer Engineering, Northwestern University, Evanston, Illinois 60208-3118
(Received 24 March 1999)

We used a spatially broadband optical parametric amplifier for image amplification. In the phase-sensitive configuration of the amplifier, we observed noiseless amplification of input images. For a gain of $\simeq 2.5$, we measured noise-figure values of (0.2 ± 0.6) and (0.4 ± 0.5) dB, respectively, for two amplifiers of different lengths. These experimental values agree with theory (for an ideal noiseless amplifier the noise figure is 0 dB) and are almost 2 dB lower than the quantum limit of an ideal phase-insensitive amplifier.

PACS numbers: 42.50.Lc, 03.67.Hk, 42.50.Dv, 42.65.Ky

The success of many precision measurements often depends on the use of amplifiers. The sensitivity of these measurements is, therefore, limited by the amount of noise that the amplifier adds to the signal. For electronic and microwave signals, the noise floor is determined by thermal fluctuations. At optical frequencies, however, the thermal noise becomes negligibly small. In that case, the noise floor of a phase-insensitive amplifier (PIA), i.e., a linear optical amplifier whose gain does not depend on the signal phase, is determined by a fundamental quantum limit [1], which arises ultimately from zero-point field fluctuations. In a typical optical amplifier, these fluctuations cause spontaneous emission of photons, resulting in added noise to the signal. For a coherent-state input, the degradation of signal-to-noise ratio (SNR) at the output approaches 3 dB for high gain. The noise owing to the zero-point fluctuations, however, can be avoided [1] by employing a proper phase-sensitive amplifier (PSA) that either amplifies or deamplifies the input signal depending on its phase. This noise-free property of the PSA is related to the fact that every act of spontaneous or stimulated emission in such a device produces a pair of correlated photons, whose quantum correlation can be utilized for noise cancellation. One has to note, however, that every signal can be represented as a superposition of two quadratures oscillating with a $\pi/2$ phase shift with respect to each other; if one quadrature is amplified in a PSA, the other must be deamplified.

The quantum correlations imposed by a PSA have been exploited to produce nonclassical states of light [2]. Recently, it was experimentally demonstrated that a PSA does not add any noise while amplifying continuous-wave [3] and pulsed [4] time-domain signals. A practical realization of a PSA is a traveling-wave optical parametric amplifier (OPA), which provides broadband gain not only in the temporal domain, but also in the spatial domain. The spatially broadband nature of the OPA suggests its potential use for noiseless amplification of spatial-domain signals, i.e., images [5], as well as for sub-shot-noise microscopy [6], cloning of quantum images [7], etc.

The spatially broadband gain of the OPA has been employed in classical imaging experiments, such as parametric up-conversion of infrared (IR) images to the visible region, edge enhancement, and time-gated image recovery [8]. In contrast to this past research on classical imaging, our work addresses the quantum-noise issues in image amplification by means of an OPA. Recently, we employed optical homodyne tomography to measure the quantum statistics of the spontaneous emission (parametric fluorescence) in the OPA, and showed that, while the photon statistics of either of the two parametric beams is thermal, their joint photon-number distribution exhibits nonclassical correlations [9]. We also measured quantum correlations between the corresponding spatial frequencies ("quantum image" [7,10]) of a parametrically amplified (signal) image and its generated conjugate (idler) image, and found the direct-detected difference noise to be $\simeq 5$ dB below the shot-noise level [11]. In this Letter, we report, to the best of our knowledge, the first observation of noiseless amplification of images by a phase-sensitive optical parametric amplifier.

The input-output transformation governing an ideal linear amplifier depends on whether it is a PIA or a PSA [1]. One has $\hat{b} = \mu\hat{a} + \nu\hat{v}^\dagger$ for PIA and $\hat{b} = \mu\hat{a} + \nu\hat{a}^\dagger$ for PSA, where $\hat{a}$ is the annihilation operator for the signal field mode, $\hat{v}$ is that for a vacuum-state mode internal to the PIA, and $|\mu|^2 - |\nu|^2 = 1$. The mean signal-output photon number $\hat{n}_b \equiv \hat{b}^\dagger\hat{b}$ with respect to an input signal in a coherent state $|\alpha\rangle$ is $\langle\hat{n}_b\rangle = \gamma|\alpha|^2 + \gamma - 1$ for PIA and $\langle\hat{n}_b\rangle = \gamma|\alpha|^2 + (\gamma - 1)(|\alpha|^2 + 1) + 2\sqrt{\gamma(\gamma - 1)}\,|\alpha|^2\cos\theta$ for PSA, where $\gamma = |\mu|^2$ and $\theta = \arg(\nu) - \arg(\mu) - 2\arg(\alpha)$. For $|\alpha|^2 \gg 1$, the parametric gain for the PIA is $G = \gamma$. On the other hand, for the PSA the mean output photon number depends on the value of θ; the maximum gain $G = 2\gamma - 1 + 2\sqrt{\gamma(\gamma - 1)}$ is achieved at $\theta = 0$. The variance of the output photon number is

$$\langle\Delta\hat{n}_b^2\rangle = G(2G - 1)\,|\alpha|^2 + G(G - 1), \quad \text{(PIA)}, \quad (1)$$

$$\langle\Delta\hat{n}_b^2\rangle = G^2|\alpha|^2 + 2\gamma(\gamma - 1), \ \text{(PSA with } \theta = 0). \quad (2)$$

We define the SNR as the ratio of the square of the mean photon number to the photon-number variance. The noise

 0031-9007/99/83(10)/1938(4)$15.00

figure (NF) of a device is the ratio of the SNR at its input to that at its output. For a coherent-state input signal field that is sufficiently bright ($|\alpha|^2 \gg 1$) to render the second terms in Eqs. (1) and (2) negligible, $\mathrm{NF}_{\mathrm{PIA}} = 2 - 1/G$ and $\mathrm{NF}_{\mathrm{PSA}} = 1$. Therefore, quantum mechanics imposes a fundamental limit on the performance of a PIA, resulting in the degradation of the SNR, which reaches a factor of 2 (3 dB) at high gains. In contrast, a PSA does not change the SNR for any value of G. Even when the coherent-state input light is so weak ($|\alpha|^2 \sim 1$) that the photon-number noise of spontaneous emission (parametric fluorescence) denoted by the second term in Eq. (2) is comparatively significant, the PSA still preserves the SNR if the signal is defined to be the appropriate field quadrature and detected by homodyne measurement [12].

Both the PIA and the PSA can be implemented in practice by using a traveling-wave OPA that is described by the following equations [2]:

$$\hat{b}_s = \mu \hat{a}_s + \nu \hat{a}_i^{\dagger}, \qquad \hat{b}_i = \mu \hat{a}_i + \nu \hat{a}_s^{\dagger}, \tag{3}$$

where $\hat{a}_s$ ($\hat{a}_i$) is the input and $\hat{b}_s$ ($\hat{b}_i$) is the output annihilation operator, respectively, for the signal (idler) field mode. When only $\hat{a}_s$ is excited at the input, the OPA works as a PIA, whereas the PSA configuration requires excitation of the $(\hat{a}_s + \hat{a}_i)/\sqrt{2}$ mode and detection of the $(\hat{b}_s + \hat{b}_i)/\sqrt{2}$ mode. Equations (3) can be easily extended to the spatially multimode case if the pump in the OPA is assumed to be a plane wave of spatial frequency $\vec{q} = 0$. In this case, the equations couple a plane-wave mode $\hat{a}_s(\vec{q})$ with $\hat{a}_i(-\vec{q})$, giving $\hat{b}_s(\vec{q})$ and $\hat{b}_i(-\vec{q})$ at the output, where $\vec{q}$, the spatial frequency in $\hat{a}_s(\vec{q})$, is the transverse component of the signal wave vector. In a typical OPA, due to phase mismatch $\Delta k(q) = k_p - k_s - k_i + (k_s^{-1} + k_i^{-1})\,|\vec{q}|^2/2$ between the interacting modes, the coefficients μ and ν are, in general, functions of $\vec{q}$ [13]. Here, k_p, k_s, and k_i are the magnitudes of the pump, signal, and idler wave vectors, respectively, and the paraxial approximation has been used. For images composed of spatial frequencies $|\vec{q}| < q_{\max}$, where $q_{\max} \sim \sqrt{k_p/l}$ [14] is the spatial bandwidth of the OPA of length l, μ, and ν are practically independent of $\vec{q}$. If μ and ν are considered constant, then the spatial Fourier transforms of Eqs. (3) lead to equations that are of the same form, but relate $\hat{a}_s(\hat{\rho})$, $\hat{a}_i(\hat{\rho})$ to $\hat{b}_s(\hat{\rho})$, $\hat{b}_i(\hat{\rho})$, i.e., they describe the input-output transformation of an image point located at the transverse spatial coordinate $\hat{\rho}$. Thus, either the phase-insensitive or phase-sensitive amplification of an image can be realized within the spatial bandwidth of the OPA.

In a realistic situation wherein the output of the OPA is direct detected with efficiency $\eta < 1$, the measured output is described by $\langle \hat{d}^{\dagger}\hat{d} \rangle$ and $\langle (\Delta \hat{d}^{\dagger}\hat{d})^2 \rangle$. Here, $\hat{d}$ is related to $\hat{b}$ through $\hat{d} = \sqrt{\eta}\,\hat{b} + \sqrt{1-\eta}\,\hat{c}$, where $\hat{c}$ is the annihilation operator of an independent vacuum-state mode that is needed to account for the fluctuations introduced by the back action of the loss due to imperfect η. Then, the total NF of the amplifier and the detection setup is given by

$$\mathrm{NF}_{\eta} = \mathrm{NF}_{\mathrm{amp}} + \frac{1-\eta}{\eta G}, \tag{4}$$

where $\mathrm{NF}_{\mathrm{amp}} = \mathrm{NF}_{\eta=1}$ is the intrinsic NF of the amplifier (PIA or PSA) as derived previously. Note that, for $G = 1$, $\mathrm{NF}_{\eta} = 1/\eta$, which is the NF of the lossy detection setup alone.

Our experimental layout is shown in Fig. 1. The OPA consists of a potassium titanyl phosphate (KTP) crystal, with a length of either 3.25 or 5.21 mm, that is pumped by an s-polarized frequency-doubled beam (532 nm) from a Q-switched, mode-locked, neodymium-doped yttrium-aluminum-garnet (Nd:YAG) laser. The laser is Q-switched at a repetition rate of 1.0 kHz. The resulting Q-switch envelopes of the pump and signal pulses are $\simeq$145 and $\simeq$200 ns in duration, respectively. The mode-locked pulses underneath these Q-switch pulse envelopes are estimated to be $\simeq$85 and $\simeq$120 ps long for the pump and signal beams, respectively. The object to be imaged is an element in a USAF test pattern, which is composed of three rectangular apertures that define its horizontal resolution. The object is illuminated by the IR beam (1064 nm) from the laser and imaged into the center of the crystal via a $\times 1$ telescope, which is made up of two 10-cm focal-length lenses. If the IR signal beam at the input of the OPA is either s or p polarized, then the amplifier operates in its phase-insensitive configuration. In our experiment, however, we make the input signal excite both the s and p modes equally, i.e., it is made polarized at a 45° angle with respect to the pump polarization, which renders the OPA phase-sensitive. The pump beam is weakly focused into the KTP crystal so that it can be approximated as a plane wave having zero spatial frequency ($\vec{q} = 0$). A dichroic beam splitter (DBS) directs the pump beam coincidentally with the zero spatial-frequency component of the image-bearing signal beam into the crystal, where the pump amplifies the image within the spatial bandwidth of the OPA. The amplified image is

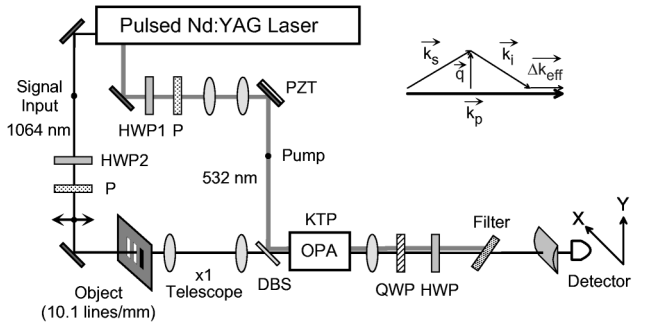

FIG. 1. Schematic of the experimental setup to measure 1D spatial profiles of the intensity and noise power of an image amplified by the traveling-wave OPA. A feedback signal to the PZT is used to lock for maximum amplification in the phase-sensitive configuration. The phase-matching diagram in terms of the spatial frequency $\vec{q}$ is shown in the upper-right corner.

subsequently magnified 24 times by a 40-mm focal-length lens that is placed after the crystal. This is to ensure that the image can be spatially resolved when scanned by an InGaAs photodetector of 300 μm diameter. After the magnifying lens, the combination of a quarter-wave plate (QWP) and a half-wave plate (HWP) is used to change the IR polarization in such a way that the transmission of the amplified IR image through a pump-blocking filter (placed at Brewster's angle) is maximized, whereas the 532 nm pump is completely absorbed. A cylindrical lens is used to compress the image in the vertical direction; the corresponding increase in intensity causes the detected optical noise of the unamplified image (pump blocked) to be $\simeq$2 dB above the electronic-noise floor of the photodetection system. The photodetector scans the image along the horizontal direction and measures the mean intensity and the 27-MHz noise power at each point, both with and without amplification. The phase of the pump beam relative to that of the signal beam is locked to maximize the parametric gain, by means of a feedback loop that drives the piezoelectric transducer (PZT).

An essential feature of our experiment is that the parametric gain of the OPA is uniform over the photodetector's bandwidth. This feature is illustrated in the inset of Fig. 2 where we plot the measured (by inserting an electro-optic modulator between the lenses of the $\times 1$ telescope in the path of the input signal beam) 27-MHz gain vs the measured dc gain for values up to $G = 4$. The equality of the two gains enables us to experimentally determine the total NF by relating the dc mean-intensity gain to the photocurrent noise-power gain at 27 MHz, by using the formula

$$\mathrm{NF} = \frac{\text{noise-power gain}}{\eta(\text{mean-intensity gain})^2}. \qquad (5)$$

Before proceeding with the NF measurements, we first experimentally determined the spatial bandwidth of the OPA for the 5.21-mm long KTP crystal. The setup for this measurement was essentially the same as the one given in Ref. [11]. The spatial frequency q was selected by adjusting the lateral position of an iris placed in the Fourier plane located midway between the input lenses that constitute the $\times 1$ telescope. By using objects with various resolutions, we measured the phase-insensitive gain for various spatial frequencies, while keeping the gain at zero spatial frequency fixed. Figure 2 shows the relevant data that were taken with the use of a single lens to focus the pump beam to a spot size of 47-μm intensity radius in the KTP crystal. It shows good agreement with the theoretical curve derived from Eq. (3) and the spatial-frequency-dependent μ and ν given in Refs. [11,13]. One can see from Fig. 2 that our OPA can effectively amplify only those images whose spatial-frequency content is limited to a narrow range near $q = 10$ lines/mm. For larger q's, amplification is limited by the spatial bandwidth of the KTP crystal; and for smaller q's, the gain is limited because the spot size of the pump beam in the KTP crystal is too small to overlap fully with the input image. By replacing the single focusing lens in the pump arm with a telescopic system composed of 5 and 10 cm focal-length lenses, we were able to increase the pump-beam intensity radius in the KTP crystal to 116 μm while still achieving phase-sensitive gains above 2 in both the crystals. In order to stay within both the spatial bandwidth and the transverse-size limits of our OPA, we chose element 3.3 of the test pattern, which has a resolution of 10.1 lines/mm. In addition, we blocked one of the rectangular apertures on one side so that the input object is a double slit with 99 μm slit separation and 50 μm slit width. Furthermore, we placed a square aperture in front of the object to limit its dimensions to $\simeq$150 μm $\times$ 150 μm.

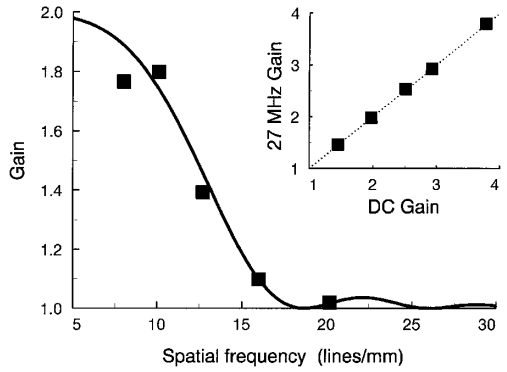

FIG. 2. Spatial bandwidth of the OPA. The solid curve is theoretical and shows the phase-sensitive gain for the qth spatial frequency, given a gain of 2 for the 0th spatial frequency. The experimental points (squares) were obtained with use of a single 40-cm focal-length lens to focus the pump beam. The inset shows linear relationship between the dc gain and the 27-MHz gain. The dotted line represents a slope of 1.

The spatial image profiles of the signal and noise scanned by the photodetector are shown in Fig. 3. The phase-sensitively amplified image shows very little spread compared to the bare image, indicating that the spatial spectrum of the image was well within the phase-matching bandwidth of the OPA. To minimize the effect of spatial averaging caused by the finite size of the photodetector, we perform the noise-figure characterization using experimental values of the intensity gain and the noise-power gain measured at the peaks of the spatial profile. Spatially broadband intensity gains of $G \simeq 2.5$ were obtained at the peaks, with the noise power being amplified at a slower rate than the square of the mean intensity. This means that the use of the phase-sensitive OPA resulted in an improvement of the detected SNR, because the SNR after amplification became less sensitive to detection and propagation losses than the SNR of the input coherent-state signal. In our setup, the overall detection efficiency was measured to be $\eta = 0.82$.

Using the gain measurements for the mean intensity and the noise power shown in Fig. 3, along with the measured value of η, we obtained from Eq. (5) the following values

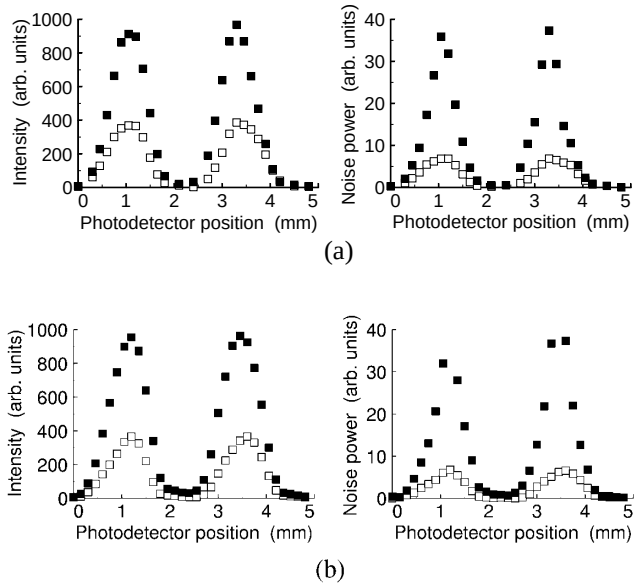

FIG. 3. 1D spatial profiles of the intensity (left) and the noise power (right) for two KTP crystals, having lengths of (a) 3.25 mm and (b) 5.21 mm. Profiles of both the unamplified (empty squares) and the amplified (full squares) images are shown.

of the total NF of the optical amplifier: (0.2 ± 0.6) dB at $G = 2.5$ for the 3.25 mm KTP crystal, and (0.4 ± 0.5) dB at $G = 2.6$ for the 5.21 mm KTP crystal. These values agree with the theoretical values predicted for the PSA, and are $\simeq 2$ dB below the predicted NF values for a PIA at the same gain and detection efficiency. Also, one obtains improvement compared to $\mathrm{NF} = -10\log\eta = 0.86$ dB for our detection setup in the absence of amplification, owing to optical preamplification before loss. The intrinsic NF of the phase-sensitive OPA is obtained from the values of the total NF using Eq. (4), which gives (-0.2 ± 0.6) dB and (0.0 ± 0.5) dB for the 3.25-mm and the 5.21-mm long crystals, respectively. These numbers agree, within the experimental margin of error, with the intrinsic NF of 0 dB predicted for the PSA, in contrast to the $2 - 1/G \simeq 2$ dB NF expected for a PIA at the same mean-intensity gain. Thus, at the peaks of the spatial profile, the SNR of the amplified image at the output of the OPA equals the SNR of the input image, i.e., our PSA performs noiseless image amplification.

In conclusion, we have used a phase-sensitive OPA to amplify a two-slit image without adding any noise, for the first time to our knowledge. We also demonstrated that optical preamplification can be used to avoid degradation of the signal-to-noise ratio of an image owing to detection and propagation losses. Our work shows that the quantum properties of a phase-sensitive optical parametric amplifier can be successfully employed for enhancing the imaging of faint objects, which adds to its classical advantages of time-gating and phase discrimination.

This work was supported in part by the U.S. Office of Naval Research.

*Email address: kumarp@nwu.edu

[1] C. M. Caves, Phys. Rev. D **26**, 1817 (1982).
[2] A. Heidmann, R. J. Horowicz, S. Reynaud, E. Giacobino, C. Fabre, and G. Camy, Phys. Rev. Lett. **59**, 2555 (1987); O. Aytür and P. Kumar, *ibid.* **65**, 1551 (1990); L.-A. Wu, H. J. Kimble, J. L. Hall, and H. Wu, *ibid.* **57**, 2520 (1986); C. Kim and P. Kumar, *ibid.* **73**, 1605 (1994); S. Schiller, G. Breitenbach, S. F. Pereira, T. Müller, and J. Mlynek, *ibid.* **77**, 2933 (1996); M. E. Anderson, D. F. McAlister, M. G. Raymer, and M. C. Gupta, J. Opt. Soc. Am. B **14**, 3180 (1997); Q. Pan, Y. Zhang, T. C. Zhang, C. D. Xie, and K. C. Peng, J. Phys. D **30**, 1588 (1997); S. F. Pereira, M. Xiao, H. J. Kimble, and J. L. Hall, Phys. Rev. A **38**, 4931 (1988); R.-D. Li, S.-K. Choi, C. Kim, and P. Kumar, *ibid.* **51**, R3429 (1995); K. Schneider, M. Lang, J. Mlynek, and S. Schiller, Opt. Expr. **2**, 59 (1998); K. Bergman, H. A. Haus, E. P. Ippen, and M. Shirasaki, Opt. Lett. **19**, 290 (1994); D. Levandovsky, M. Vasilyev, and P. Kumar, *ibid.* **24**, 984 (1999).
[3] Z. Y. Ou, S. F. Pereira, and H. J. Kimble, Phys. Rev. Lett. **70**, 3239 (1993).
[4] J. A. Levenson, I. Abram, Th. Rivera, and Ph. Grangier, J. Opt. Soc. Am. B **10**, 2233 (1993).
[5] M. I. Kolobov and L. A. Lugiato, Phys. Rev. A **52**, 4230 (1995).
[6] M. I. Kolobov and P. Kumar, Opt. Lett. **18**, 849 (1993).
[7] A. Gatti, H. Wiedemann, L. A. Lugiato, I. Marzoli, G.-L. Oppo, and S. M. Barnett, Phys. Rev. A **56**, 877 (1997); I. Marzoli, A. Gatti, and L. A. Lugiato, Phys. Rev. Lett. **78**, 2092 (1997); A. Gatti, L. A. Lugiato, G.-L. Oppo, R. Martin, P. D. Trapani, and A. Berzanskis, Opt. Expr. **1**, 21 (1997); K. I. Petsas, A. Gatti, and L. A. Lugiato, Quantum Semiclass. Opt. **10**, 789 (1998).
[8] See E. Lantz and F. Devaux, Quantum Semiclass. Opt. **9**, 279 (1997), and references therein; F. Devaux, E. Guiot, and E. Lantz, Opt. Lett. **23**, 1597 (1998).
[9] M. Vasilyev, S.-K. Choi, P. Kumar, and G. M. D'Ariano, Opt. Lett. **23**, 1393 (1998); in Proceedings of the OSA Annual Meeting, 1998 (Report No. ThZZ3).
[10] D. V. Strekalov, A. V. Sergienko, D. N. Klyshko, and Y. H. Shih, Phys. Rev. Lett. **74**, 3600 (1995).
[11] M. L. Marable, S.-K. Choi, and P. Kumar, Opt. Expr. **2**, 84 (1998).
[12] H. P. Yuen, Opt. Lett. **12**, 789 (1987).
[13] A. Gavrielides, P. Peterson, and D. Cardimona, J. Appl. Phys. **62**, 2640 (1987).
[14] M. I. Kolobov and I. V. Sokolov, Sov. Phys. JETP **69**, 1097 (1989).